Published by Institute of Physics Publishing for SISSA/ISAS
Received: *December 16, 2002*
Revised: *April 24, 2003*
Accepted: *April 25, 2003*

Geometric dualities in 4d field theories and their 5d interpretation

Sebastián Franco and Amihay Hanany[*]

Center for Theoretical Physics, Massachusetts Institute of Technology
Cambridge, MA 02139, USA
E-mail: sfranco@mit.edu, hanany@mit.edu

Abstract: We study four-dimensional $\mathcal{N} = 1$ gauge theories arising on D3-branes probing toric singularities. Toric dualities and flows between theories corresponding to different singularities are analyzed by encoding the geometric information into (p, q) webs. A new method for identifying quiver symmetries of the four-dimensional theories using the brane webs is developed. Five-dimensional theories are associated to the theories on the D3-branes by using (p, q) webs. This leads to a novel interpretation of Seiberg duality, which can be mapped to the crossing of curves of marginal stability in five dimensions.

Keywords: Duality in Gauge Field Theories, Conformal Field Models in String Theory, Brane Dynamics in Gauge Theories.

[*]Research supported in part by the CTP and the LNS of MIT and the U.S. Department of Energy under cooperative agreement #DE-FC02-94ER40818. A.H. is also supported by the Reed Fund Award and a DOE OJI award.

JHEP04(2003)043

Contents

1. Introduction

String theory has been widely used to study the dynamics of gauge theories. In doing so, it sometimes provides a completely new interpretation of field theory results. The relation goes in both directions, and gauge theories can be used to understand string theory processes. The main ingredient in this connection is the fact that the low energy dynamics of D-branes is described by SYM on their world volume, with different amounts of supersymmetry depending on the specific configuration. Several ways of constructing gauge theories using D-branes have been developed. The main strategies employed are brane setups [1], geometric engineering [2] and brane probes [3].

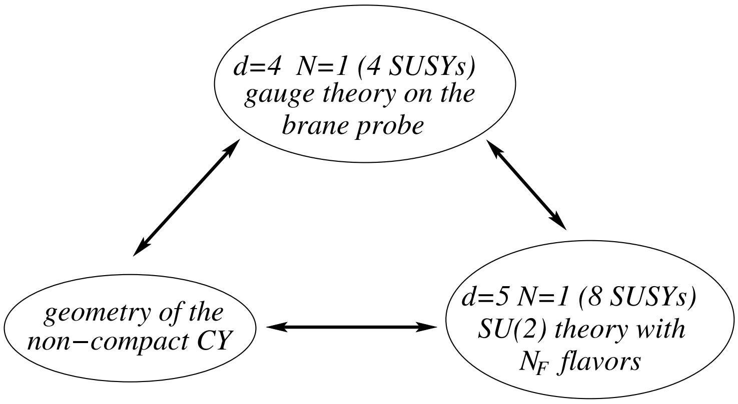

Figure 1: The three alternative perspectives that will be developed in this paper. The connections between them will be made using (p, q) webs.

Toric duality was discovered while studying the gauge theories arising on D-branes probing toric singularities. The classical moduli space of a D-brane on a singularity is exactly the probed geometry [4]. In [5, 6], it was discovered that given a toric singularity, the corresponding gauge theory is not unique. The different phases associated to a singularity form equivalence classes of $\mathcal{N} = 1$ four dimensional models that describe the same physics in the IR limit. In [7, 8, 11], it was shown that toric duality is Seiberg duality. In this way, highly non-trivial sets of dual theories were constructed, and Seiberg duality acquired a fully geometric interpretation in string theory.

The purpose of this paper is to look at gauge theories living on D3-branes probing toric singularities from three completely different perspectives, studying not only the transition between toric dual theories but also the flow between theories corresponding to different geometries. These complementary approaches are summarized in figure 1, and we will discuss how different physical processes manifest in the three languages. In the first place, we will study directly the $\mathcal{N} = 1$ theories in $d = 4$. In this context, toric duals are related by Seiberg dualities, while theories for different geometries correspond to (un)higgsings. The second viewpoint is purely geometric, and the continuous flow between theories is achieved by blow-ups and blow-downs of the corresponding non-compact Calabi-Yau. Finally, every theory under study has an associated five dimensional $\mathcal{N} = 1$, SU(2) partner.[1] The correspondence follows from considering M theory on the different CY threefolds. In this language, there exist a one to one mapping between the change of parameters that interpolates between four dimensional toric dual theories and the change of the BPS spectrum in five dimensions (crossing of curves of marginal stability). The key objects interconnecting these three descriptions are (p, q) webs.

The organization of this paper is as follows. In section 2, we review the main concepts of (p, q) web constructions and toric geometry. In section 3, we explain how to extract the quiver for the four dimensional theory that appears in the world volume of D3-branes

[1]Five dimensional $\mathcal{N} = 1$ theories have 8 supercharges. This is the number of SUSYs that is preserved by the (p, q) web configuration when condition (2.2) is satisfied.

probing a toric variety whose toric data is encoded in a given (p, q) web. Section 4 is devoted to understanding the flow between toric duals and theories associated to different singularities as geometric transitions and (un)higgsings. Section 5 shows the full power of (p, q) webs in establishing quiver symmetries of the four dimensional gauge theories. In section 6, we use the mapping from (p, q) webs to five dimensional theories to introduce a third perspective for toric duality and geometric transitions, namely there is a one to one correspondence between the continuous change of parameters and subsequent flops in (p, q) webs which is associated to toric duality and a change in the five dimensional BPS spectrum.

2. A review of (p, q) webs and toric geometry

2.1 (p, q) webs and five dimensional theories

In [13, 14] (p, q) webs were introduced as brane constructions to study five dimensional theories. They are type-IIB string theory configurations in which 5-branes share four spatial directions and time. The remaining dimension of the 5-branes world volumes lie on a plane parametrized by the (x, y) coordinates. Every (p, q) web can be associated to a $\mathcal{N} = 1$ gauge theory living in the $4 + 1$ dimensions common to all the 5-branes. Each brane has a (p, q) charge which is related to its tension

$$T_{p,q} = |p + \tau q| T_{D_5} \tag{2.1}$$

and to its slope

$$\Delta x : \Delta y = p : q \tag{2.2}$$

where T_{D_5} is the D5-brane tension and τ is the complex scalar of type IIB (which we have chosen equal to i in (2.2)). The last condition assures that 1/4 of the SUSYs is preserved. Branes can join at vertices, where (p, q) charge is conserved,

$$\sum_i p_i = \sum_i q_i = 0 \tag{2.3}$$

where the sum is performed over all the branes ending at a given vertex. It is easy to see that (2.1), (2.2) and (2.3) imply the equilibrium of the web.

These theories were thoroughly studied in [14]. We will give here a brief explanation on how the five dimensional parameters can be read off from the (p, q) webs. All along this paper we will deal with SU(2) theories, so we choose an SU(2) model with one flavor to exemplify all the relevant concepts (figure 2). Color branes are finite parallel branes (depicted in red in the figure). Their separation is parametrized by the expectation value of a U(1) scalar ϕ. For $\phi = 0$, both color branes coincide and we have an unbroken SU(2) gauge symmetry. When $\phi > 0$, SU(2) is broken down to U(1) and the W gauge boson gets a mass $m_W = \phi$. The bare value of the gauge coupling is given by the length of the color branes when $\phi = 0$ (see figure 2)

We can add a flavor to this theory. This is represented by a semi-infinite brane parallel to the color branes (green brane in figure 2). For $\phi = 0$ this brane corresponds to a quark

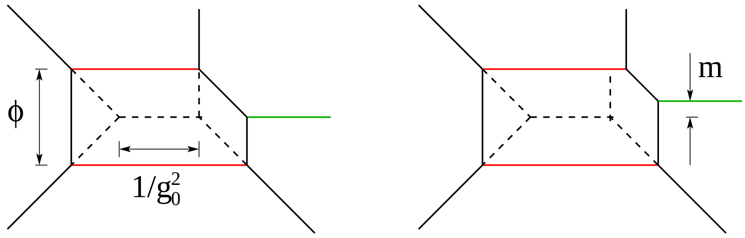

Figure 2: A (p, q) web corresponding to an SU(2) theory with one flavor.

multiplet in the **2** representation of SU(2). When ϕ grows, the gauge group is higgsed to U(1) and the **2** gives rise to two quark states with $m_{1,2} = \phi/2$. A bare mass for the quarks can be introduced by displacing the flavor brane with respect to the middle position between the color branes. In this case, the quark masses become $m_{1,2} = |m \pm \phi/2|$.

BPS saturated states correspond to string webs ending perpendicularly on the five branes. The rules governing the construction of string webs are identical to the ones we discussed for brane webs. The monopole tension is calculated as the area of the closed face of the web. The masses of BPS states and the monopole tension can be expressed in terms of ϕ, g_0 and the quark bare masses.

2.2 Toric geometry

Toric geometry and (p, q) webs are closely related. Toric geometry studies varieties that admit a $\mathrm{U}(1)^d$ action, in general with fixed points (for a complete treatment look at [17]). These spaces are described by specifying shrinking cycles and relations between them. An alternative description of this geometries is in terms of (p, q) webs. It is possible to see that the connection between both descriptions consists simply in that the brane web is a representation of the toric skeleton (for a complete discussion of the relation see [15]).

In this paper we will focus on cones over two complex dimensional toric varieties. They can be understood as T^2 fibrations over $\mathbb{C}$. Lines and vertices in the web represent fixed points of the U(1) actions (i.e. places where the fibration becomes degenerate). Lines correspond to vanishing 1-cycles, while points describe vanishing 2-cycles. The process of blowing-up a point in a given variety consists of replacing it by a 2-sphere. The toric representation of a 2-sphere is a segment. Then we see that if the points we choose to blow up are vertices in the web, we just have to replace them by segments.

We conclude this brief introduction by developing the toric representation for a specific case, the zeroth Hirzebruch surface F_0. F_0 is equal to $\mathbb{P}^1 \times \mathbb{P}^1$, so we can think about it as a 2-sphere fibered over another 2-sphere. This representation is shown in figure 3*a*. Now we want to interpret this geometry as a T^2 fibration over $\mathbb{C}$. A natural way to do this is by associating the vertical positions $y_{1,2}$ on the two 2-spheres to the two coordinates in the complex plane. Then, we associate to every point on $\mathbb{C}$ a 2-torus given by the product of the two circles parallel to the equators at the corresponding y_i. The full construction is presented in figure 3*b*. The C_2 circle vanishes at the north and south poles of the small sphere, represented torically by the two vertical lines. Analogously, the two horizontal lines

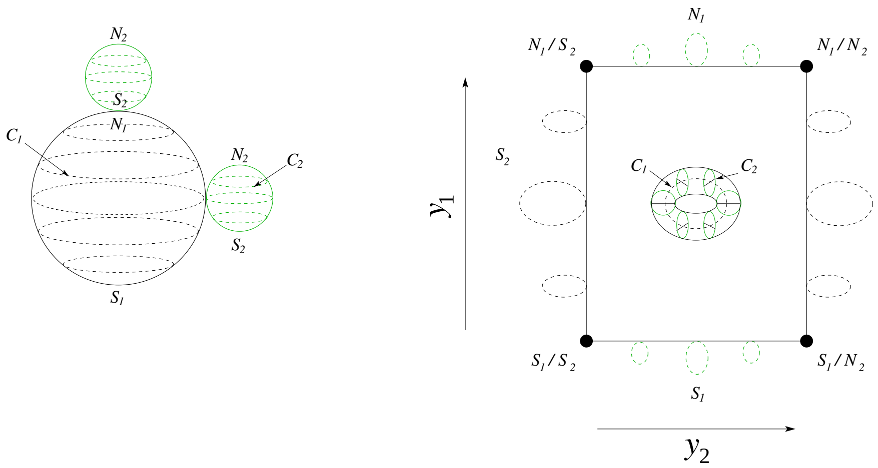

Figure 3: Toric representation of $F_0 = \mathbb{P}^1 \times \mathbb{P}^1$.

correspond to the north and south poles of the big sphere. Both C_1 and C_2 vanish at the four vertices of the rectangle. From this discussion we also see that the sizes of the different compact 2-cycles are given by the lengths of the segments in the toric skeleton.

3. Four dimensional quivers from (p, q) webs

Let us study how to obtain the quiver for the four dimensional $\mathcal{N} = 1$ theory that appears on the world volume of a D3-brane probing the type of singularities we are considering. A possible approach consists of obtaining the singularity as a partial resolution of an abelian orbifold, whose associated gauge theory is well understood. This approach was pursued in [5] and further developed in [6, 8, 9] to get the theories for the zeroth Hirzebruch and the toric del Pezzo surfaces as partial resolutions of $\mathbb{C}^3/(\mathbb{Z}_3 \times \mathbb{Z}_3)$.

A second alternative exploits the geometric information encoded in the (p, q) web. Each factor of the gauge group is given by a fractional brane, which is a bound state of D3, D5 and D7-branes. D3-branes span the four directions transverse to the singularity and thus are located at 0-cycles inside the toric variety. Analogously, D5-branes wrap 2-cycles and D7-branes wrap the compact 4-cycle. Some possible configurations are sketched in figure 4. The mirror type-IIA geometries associated to these models were studied in [16]. It was found there that 0, 2 and 4-cycles map to 3-cycles, and D3-branes become D6-branes wrapping a $\mathcal{T}^3$. The bifundamental matter content is given by the intersection matrix of the 3-cycles. Furthermore, each 3-cycle S_i wraps a 1-cycle C_i of a smooth elliptic fiber that becomes degenerate at some point z_i. Each C_i carries a (p_i, q_i) charge, and the intersection numbers for the 3-cycles can be calculated as

$$^{\#}(S_i \cdot S_j) = {}^{\#}(C_i \cdot C_j) = \det \begin{pmatrix} p_i & q_i \\ p_j & q_j \end{pmatrix} \tag{3.1}$$

The (p, q) charges of the 1-cycles are those of the external legs of the web. This suggests a profound connection between the (p, q) web and the gauge theory in four dimensions.

JHEP04(2003)043

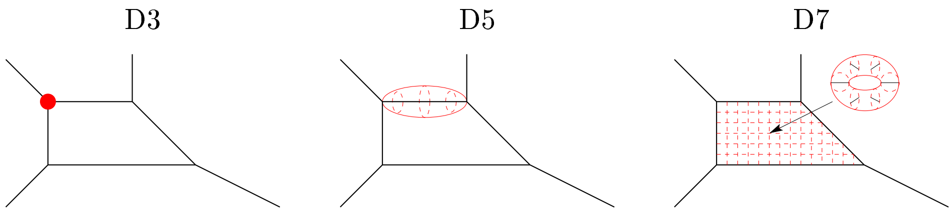

Figure 4: Possible D3, D5 and D7-branes located at 0-cycles and wrapping compact 2 and 4 cycles, respectively.

Each node in the web corresponds to the fractional brane of one gauge group factor. The external leg associated to it gives the (p,q) charges of the 1-cycle in the mirror manifold used to compute the matter content using the intersections with other 1-cycles.

As it has already been noticed in [16], (p,q) charge conservation at every node of the web ($\sum_i (p_i,q_i) = 0$) guarantees the absence of anomalies in the four dimensional gauge theory. This is the case if every node of the quiver has same number of incoming and outcoming arrows. Choosing the i-th node, we have

$$\begin{aligned} N_{in}^{(i)} - N_{out}^{(i)} &= \sum_{j\neq i} \det \begin{pmatrix} p_i & q_i \\ p_j & q_j \end{pmatrix} = \sum_{j\neq i} (q_i p_j - p_i q_j) \\ &= q_i \sum_{j\neq i} p_j - p_i \sum_{j\neq i} q_j = -q_i p_i + q_i p_i = 0\,. \end{aligned} \tag{3.2}$$

Thus we see that the theory is anomaly free.

We conclude this section with an explicit example of how the quiver theory is constructed from the brane web. We consider the case of dP_1. A possible (p,q) web for this geometry is presented in figure 5.

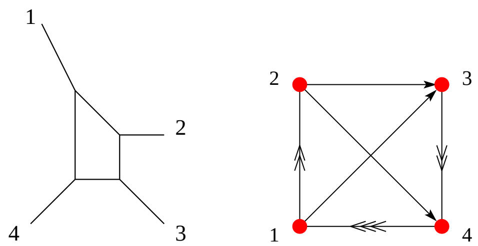

Figure 5: A (p,q) web for dP_1 and its associated quiver.

We read the (p,q) charges of the 1-cycles from the external legs of the web. They are

$$\begin{aligned} (p_1,q_1) &= (-1,2) \qquad & (p_2,q_2) &= (1,0) \\ (p_3,q_3) &= (1,-1) \qquad & (p_4,q_4) &= (-1,-1)\,. \end{aligned} \tag{3.3}$$

Using (3.1), it is immediate to calculate the intersection numbers

$$\begin{aligned} \#(C_1.C_2) &= -2 \qquad & \#(C_1.C_3) &= -1 \qquad & \#(C_1.C_4) &= 3 \\ \#(C_2.C_3) &= -1 \qquad & \#(C_2.C_4) &= -1 \qquad & \#(C_3.C_4) &= -2\,. \end{aligned} \tag{3.4}$$

The resulting quiver is presented in figure 5, where we have explicitly labeled the nodes according to the associated external legs.

4. Geometric transitions

In what follows, we will apply the observations in sections 2 and 3 to obtain the phases of F_0 and of all del Pezzo surfaces up to dP_3. We will use (p,q) web diagrams as representations of the probed geometries and will study which are the resulting theories after successive blow-ups and blow-downs. This method proves to be very powerful and gives all the phases associated to different singularities without doing any calculation!

4.1 Blow-ups, unhiggsing and (p,q) webs

Del Pezzo surfaces are constructed by blowing-up up to eight generic points on P^2. When the number of blown up points is less or equal to three, the $\mathrm{SL}(3,\mathbb{C})$ symmetry of P^2 can be used to map the generic positions of these points to any desired location. In particular, these can be chosen to be vertices of the web configuration. Thus, all possible blow-ups of up to three points can be studied by blowing-up vertices of the web. Using the (p,q) web description of a sphere, the blow-up of a point is obtained by replacing it by a segment. The (p,q) charges of the two external legs at the endpoints of the blown-up 2-cycle are given by the charges of the original external leg.

The inverse process, a blow-down of a compact 2-cycle to a point, is given in the (p,q) web description by the replacement of a segment by a point, and the subsequent combination of the external legs attached at the end points of the segment. For the four dimensional gauge theory this process is simply a higgsing of the U(1) groups associated to both external legs to the linear combination of them under which the bifundamental field that gets a non-zero vev is neutral.

Let us use this method to calculate all the phases associated to D3-branes probing cones over toric del Pezzo surfaces. The starting point is a (p,q) web describing dP_0 (figure 6). We have identified in red the branes obtained as a result of a blow-up. Once we have the resulting webs, we can calculate the intersection matrix and the quiver as in (3.1). The three webs in figure 6 are related by $\mathrm{SL}(2,\mathbb{Z})$ transformations, and describe the only phase of dP_1.

The following step is taking any of the equivalent webs for dP_1 (what we obtain is independent of our choice) and perform all possible blow-ups. The results are shown in

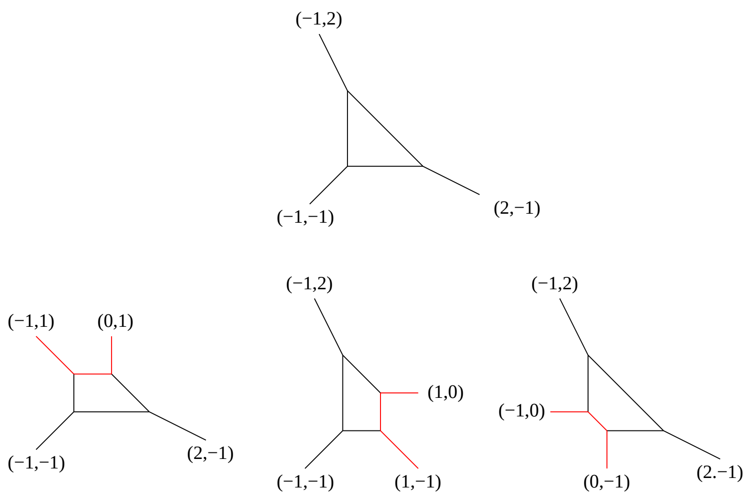

Figure 6: Possible blow-ups of dP_0. All the resulting theories are equivalent.

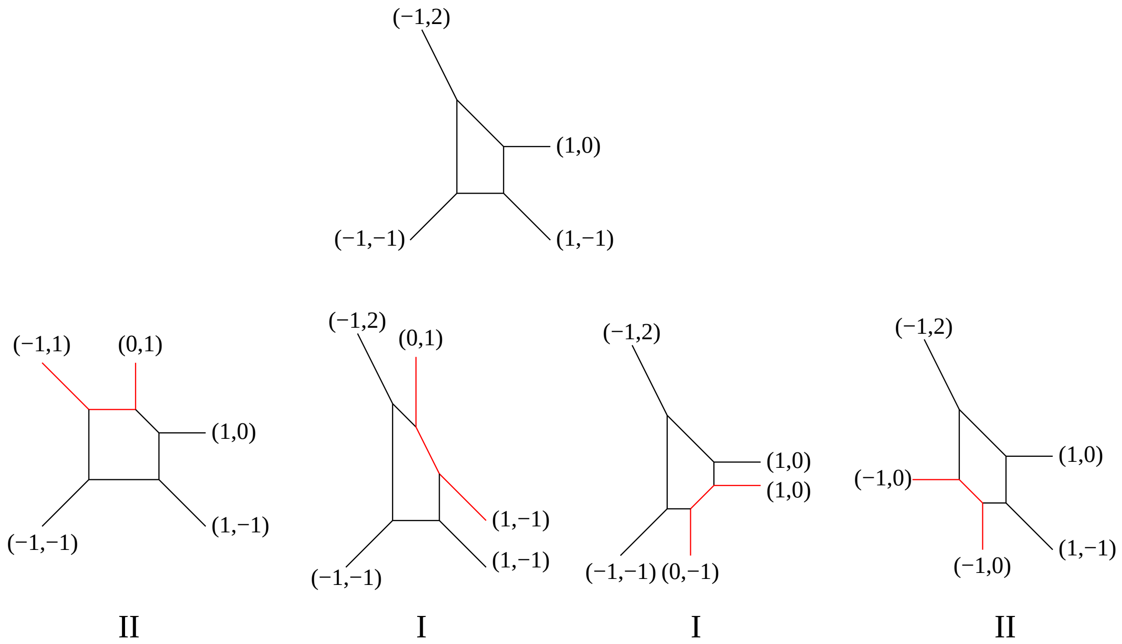

Figure 7: Possible blow-ups of dP_1. They correspond to two inequivalent phases.

figure 7. After calculating the associated quivers we conclude that these webs represent two different theories. These are exactly the two toric dual models encountered in [6] for dP_2. At this point a new feature, which will persist for other geometries, appears: the existence of (p, q) webs with parallel external legs. These models are completely sensible as long as the 4d gauge theories are concerned. However, these theories present problematic issues when a 5d interpretation of the webs is intended. They may exhibit a leakage of 5d global charges due to states corresponding to strings stretching between parallel branes, and can also have directions in the moduli space along which the superpotential is not convex [14]. These drawbacks can be eliminated by providing a suitable UV completion of the theories, embedding them into larger (p, q) webs.

We now move on, take one representative for each phase of dP_2 and proceed to blow-up points. At this point, it is not possible to blow-up any vertex in the web, since in some cases this would lead to crossing external legs (additional compact 4-cycles). The theories coming from the first phase and second phase of dP_2 are presented in figures 8 and 9. Computing the quivers we obtain the four toric phases of dP_3 [7, 8].

The $\mathrm{SL}(3, \mathbb{C})$ freedom is exhausted after blowing up three points on $\mathbb{P}^1$. Thus, we cannot map a further generic point to a vertex of the web and then blow it up. This is a manifestation of the fact that dP_n surfaces do not admit a toric description beyond $n = 3$. Nevertheless, we can study the theories obtained from dP_3 after a non-generic toric blow-up. We summarize the possibilities in figure 10. These (p, q) webs define two quiver theories that are studied in detail in [22].

We close this section by emphasizing that different Seiberg dual phases can be understood as related by blowing-down a 2-cycle and blowing-up a point. This is nothing

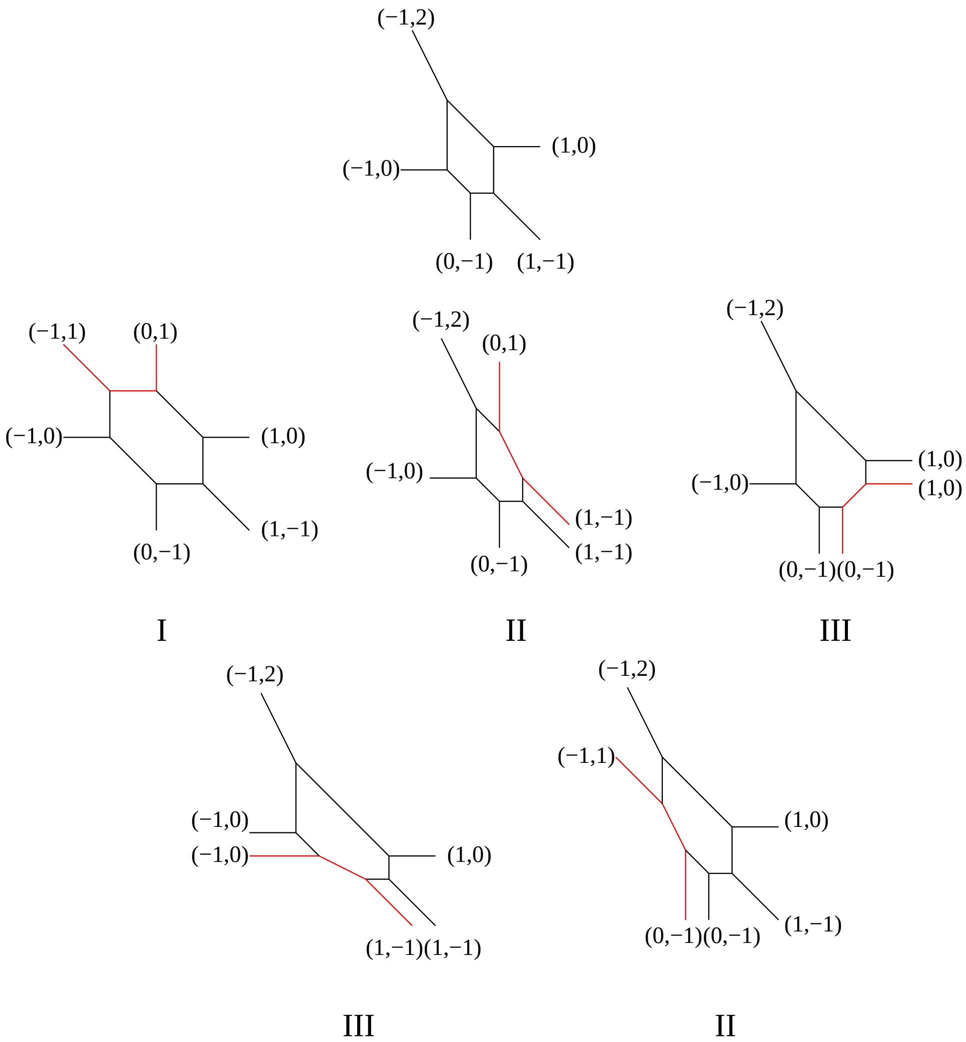

Figure 8: Possible blow-ups of phase I of dP_2.

more than an $\mathrm{SL}(3,\mathbb{C})$ transformation relocating one of the blown-up point in $\mathbb{P}^2$. In this way, the set of Seiberg duality transformations (that do not change the rank of the gauge groups, keeping them all equal) G_S satisfies

$$G_S \subset \frac{\mathrm{SL}(3,\mathbb{C})}{\mathrm{SL}(2,\mathbb{Z})}\,. \tag{4.1}$$

The quotient by $\mathrm{SL}(2,\mathbb{Z})$ eliminates those transformations that trivially do not change the intersection matrix, not leading to a dual phase. Furthermore we see that, since there are elements in $\mathrm{SL}(3,\mathbb{C})$ that do not preserve the intersection numbers, some singularities can be represented by both (p,q) webs with parallel legs and by (p,q) webs without them.

4.2 The two phases of F_0

The techniques introduced in section 4.1 can be used to study, for another example, how different phases and singularities are interconnected by the geometric processes of blowing-

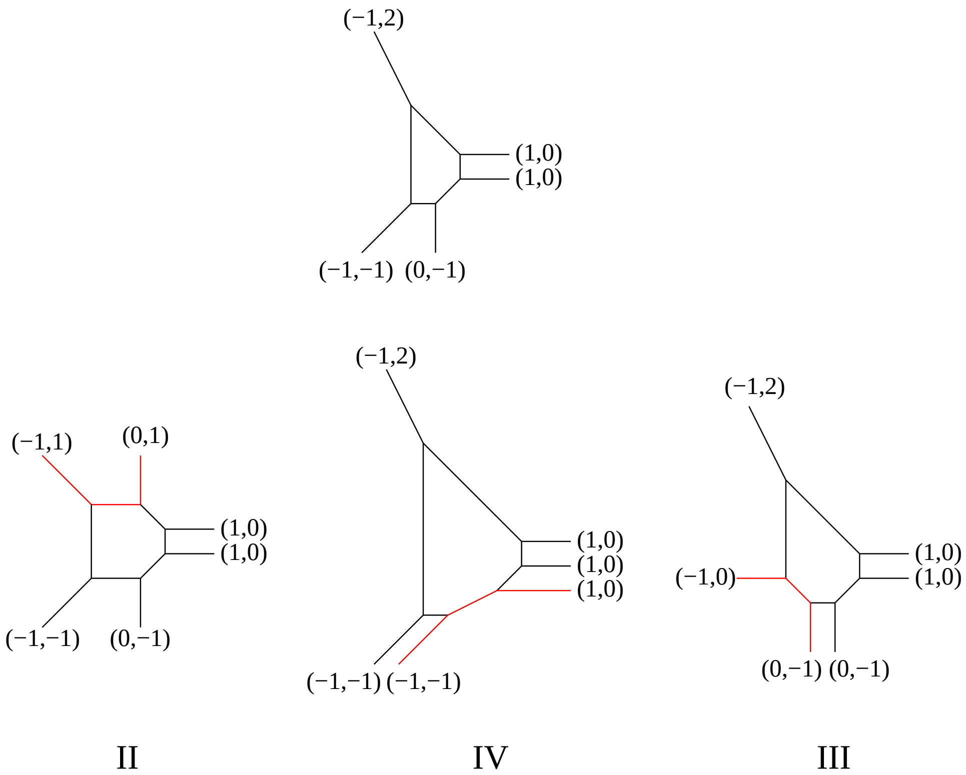

Figure 9: Possible blow-ups of phase II of dP_2.

up points and shrinking 2-cycles. In figure 11 we present a possible path connecting the two phases of F_0. Starting from phase I, we blow up two points, arriving at model II of dP_3. The last step in the flow consists of shrinking two 2-cycles to zero size, combining the corresponding external legs.

The intersection matrices for both phases can be computed using (3.1), and are presented in the appendix.

4.3 Higgsings as blow-downs

We have mentioned in section 4.1 that blow-ups of the geometry correspond to unhiggings when we look at them from the perspective of the four dimensional gauge theory on the world volume of the brane probing the singularity. Conversely, the blow-down of a compact 2-cycle to a point translates into the higgsing of two U(1) factors to a single U(1) by giving a non-zero expectation value to a bifundamental chiral field.

As we have discussed, compact 2-cycles are represented by the internal finite segments of the (p, q) web, their length given by the volume of the corresponding P^1's. Thus, we see the beautiful interplay between the two descriptions of the process. When blowing-down, we reduce the length of a segment. When this length vanishes, the external legs that are located at its endpoints are combined, adding their (p, q) charges. The two original U(1)'s merge into a single one. The resulting linear combination depends on the relation between

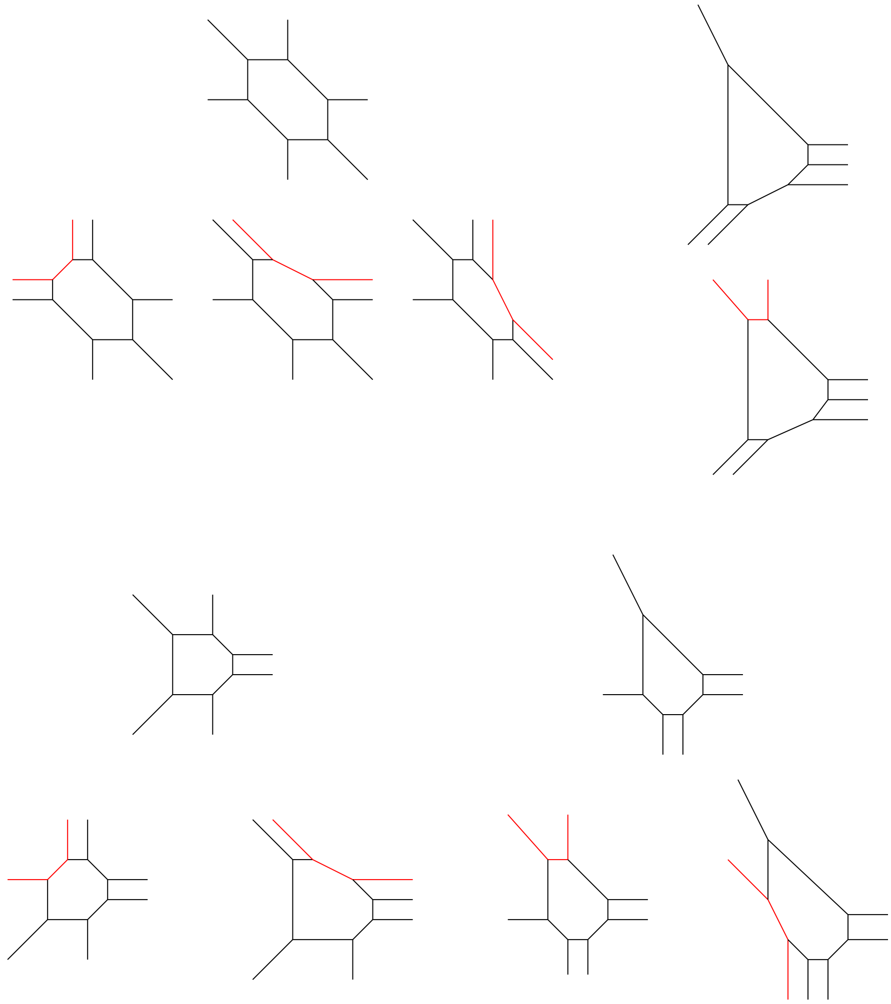

Figure 10: Possible blow-ups of the four phases of dP_3 at non-generic points. We have suppressed (p, q) charges for simplicity.

the coupling constants and is such that a bifundamental field charged under the original gauge groups is neutral with respect to it.

The (p, q) description of the original and final geometries allows an immediate identification of which vev we have to turn on in the gauge theory in order to flow down to the desired theory. Furthermore, it supplies a correspondence between gauge groups in the original and final theories. An explicit example of a blow-down from dP_3 to dP_2 will help to clarify these concepts. Let us connect the transition between the theories in figure 12. From the respective webs, we already see that they are related by the combination of nodes 2 and 3.

Before going on, let us notice that we have represented both quivers in a way that makes their symmetries explicit. The identification of these symmetries is immediate following the rules that will be presented in section 5. Theory A has a $\mathbb{Z}_2 \times \mathbb{Z}_2$ node symmetry. The first $\mathbb{Z}_2$ interchanges nodes 3 and 4. The second $\mathbb{Z}_2$ acts as a π rotation around the (34) axis

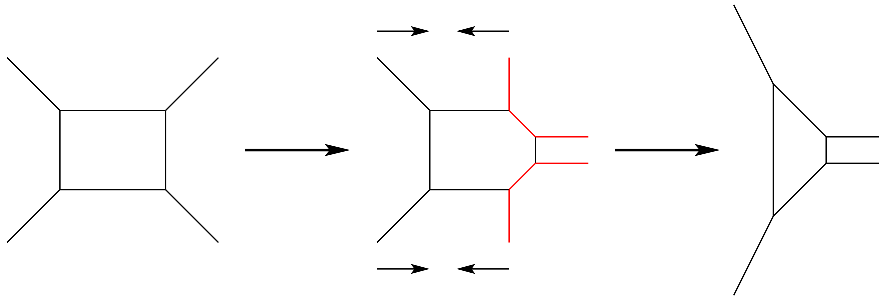

Figure 11: A possible transition between the two phases of F_0, by blowing-up two points and blowing-down two 2-cycles.

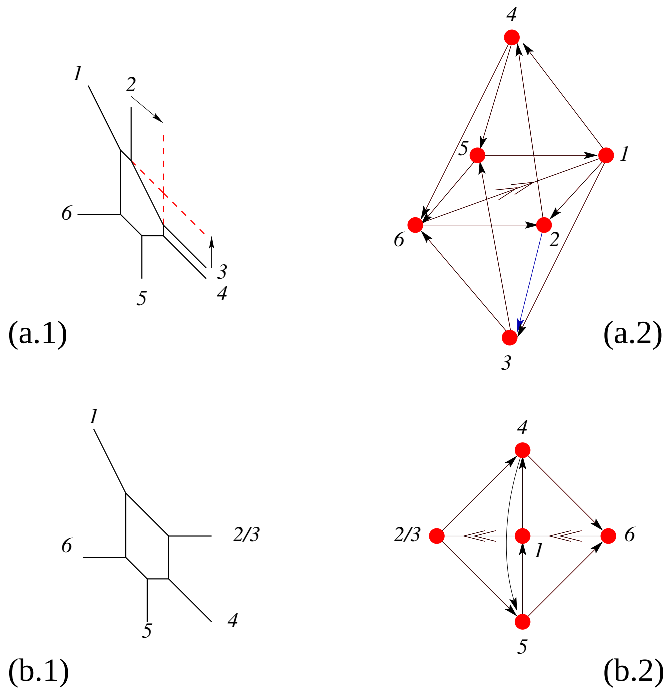

Figure 12: Higgsing from dP_3 (a.1) to dP_2 (b.1) by blowing down a 2-cycle. Their corresponding quivers are a.2 and b.2.

and a charge conjugation of all fields. These two symmetries disappear when we combine 2 and 3, but a new $\mathbb{Z}_2$ symmetry that interchanges $2/3 \leftrightarrow 6$, $4 \leftrightarrow 5$ and charge conjugate all fields appears in model B. At this point we can calculate the intersection matrices and see that theory A has 14 fields, while theory B has 11. One of the missing fields is the one getting a non-zero vev, so we can already see that masses for two fields will be generated when higgsing (notice that we know that this mass term will appear without looking at any superpotential!).[2]

[2]It is indeed very simple to understand how these two fields acquire masses. In the brane web language, the combined 2/3 leg is parallel to the existing 6, making the original ϕ_{62} and ϕ_{36} disappear. This is due to the existence of a $(\phi_{62}\phi_{23}\phi_{36})$ cubic term in the superpotential, which becomes a mass term after giving

The original superpotential is [5, 6]

$$\begin{aligned} W_A = &\ \phi_{62}\phi_{24}\phi_{46} + \phi_{51}\phi_{14}\phi_{45} - \phi_{62}\phi_{23}\phi_{36} - \phi_{51}\phi_{13}\phi_{35} + \phi_{13}\phi_{36}\phi_{61} + \\ &+ \phi_{14}\phi_{46}\tilde{\phi}_{61} + \phi_{23}\phi_{35}\phi_{56}\tilde{\phi}_{61}\phi_{12} - \phi_{24}\phi_{45}\phi_{56}\phi_{61}\phi_{12}\,. \end{aligned} \tag{4.2}$$

The combination of legs 2 and 3 corresponds to turning on a non-zero vev for ϕ_{23} in (4.2). When doing so, $\mathrm{U}(1)^{(2)} \times \mathrm{U}(1)^{(3)}$ is broken down to a single U(1), under which ϕ_{23} is neutral. At the same time two fields, ϕ_{62} and ϕ_{36}, become massive as predicted. We are interested in the IR limit of this theory, so we integrate them out using their equations of motion. Setting $<\phi_{23}>=1$, the resulting superpotential is

$$\begin{aligned} W = &-\phi_{51}\phi_{13}\phi_{35} + \phi_{51}\phi_{14}\phi_{45} + \phi_{14}\phi_{46}\tilde{\phi}_{61} + \phi_{35}\phi_{56}\tilde{\phi}_{61}\phi_{12} + \\ &+ \phi_{13}\phi_{24}\phi_{46}\phi_{61} - \phi_{24}\phi_{45}\phi_{56}\phi_{61}\phi_{12} \end{aligned} \tag{4.3}$$

which is exactly the superpotential of the dP_2 theory under consideration [5, 6].

4.3.1 An application, partial resolutions of $\mathbb{C}^3/(\mathbb{Z}_3 \times \mathbb{Z}_3)$

In sections 4.1 and 4.2, we obtained all the gauge theories associated to blow-ups of $\mathbb{P}^2$ and $\mathbb{P}^1 \times \mathbb{P}^1$ in a constructive way, identifying at every step the possible geometric blow-ups. On the other hand, in section 4.3 we traced the connection between blow-downs, higgsings and transformations of the (p, q) webs. Let us now consider an example where all these tools and ideas converge.

The four phases of dP_3 were presented in section 4.1. Furthermore, we have associated specific (p, q) webs to each of them. These theories were obtained in [7, 8] by the method of partial resolution of $\mathbb{C}^3/(\mathbb{Z}_3\times\mathbb{Z}_3)$. Let us see how these results can be recovered immediately using our techniques. The starting point is the (p, q) web for $\mathbb{C}^3/(\mathbb{Z}_3 \times \mathbb{Z}_3)$ (figure 13). In each case, we easily see which external legs have to be combined in order to get the desired phase. This is not the end of the story, the web construction also tells which fields have to get a non-zero vev in the original theory, they are the fields associated to the non-vanishing intersections of the combined 2-cycles. We summarize our results in figure 13, indicating the scalars that get a non-zero expectation value.

5. Symmetries of the four dimensional gauge theory

An appealing feature of the (p, q) language is that it makes quiver symmetries of the gauge theory evident. We will consider here two examples of how this symmetries manifest in the brane representation. These symmetries have been studied in [8, 9], along with their importance as a tool for determining the structure of superpotentials.

a non-zero expectation value to ϕ_{23}. However, the reader should be aware that the general situation is that not all gauge invariant operators permitted by a given $(p.q)$ web (alternatively by its associated quiver) appear in the corresponding superpotential.

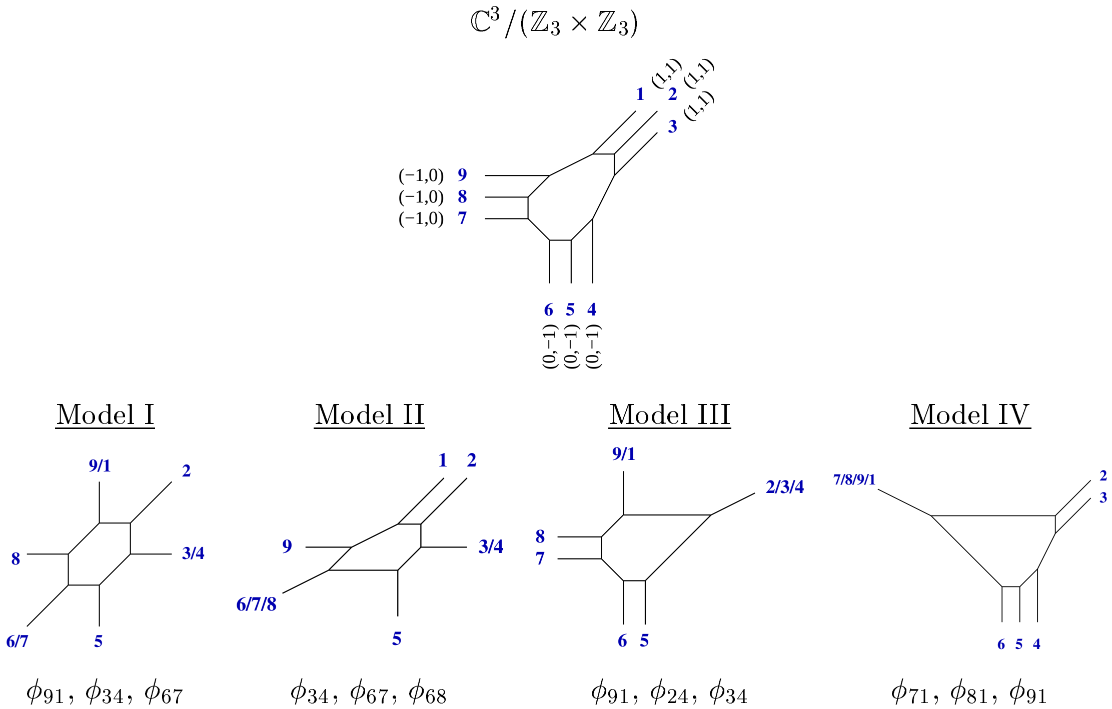

Figure 13: The four dP_3 phases obtained as partial resolutions (higgsings) of $\mathbb{C}^3/(\mathbb{Z}_3 \times \mathbb{Z}_3)$. We indicate the scalars that get a non-zero vev in each case.

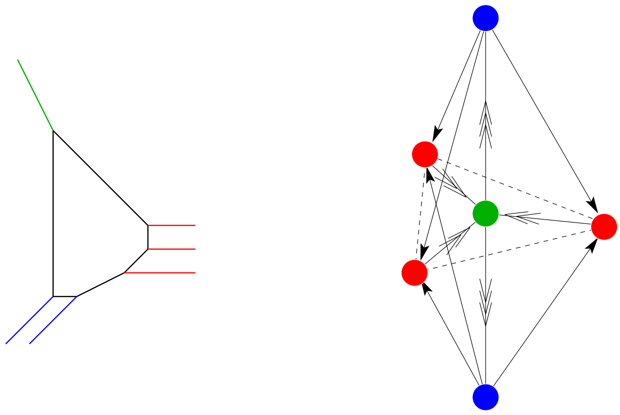

Figure 14: (p, q) web for phase IV of dP_3. We have colored the external branes giving rise to the different U(1) factors accordingly to their transformation properties under quiver symmetries.

S_n **symmetries:** these symmetries appear when the web brane configuration has sets of n parallel external legs (in the geometric language non-compact 2-cycles with the same (p, q) charges). Parallel branes have vanishing mutual intersections, while their intersections with the rest of the branes are identical. Due to this identity of the intersections, the gauge groups associated to parallel legs can be permuted leaving the quiver invariant. The symmetry group in this case is the full S_n permutation group. These discrete symmetries get enhanced to a continuous SU(n) when the parallel branes coincide. In figure 14 we show phase IV of dP_3 as an example. The three parallel red legs give rise to a S_3 symmetry between red nodes in the quiver, while there is a $\mathbb{Z}_2$ symmetry that interchanges blue nodes coming from the parallel blue branes.

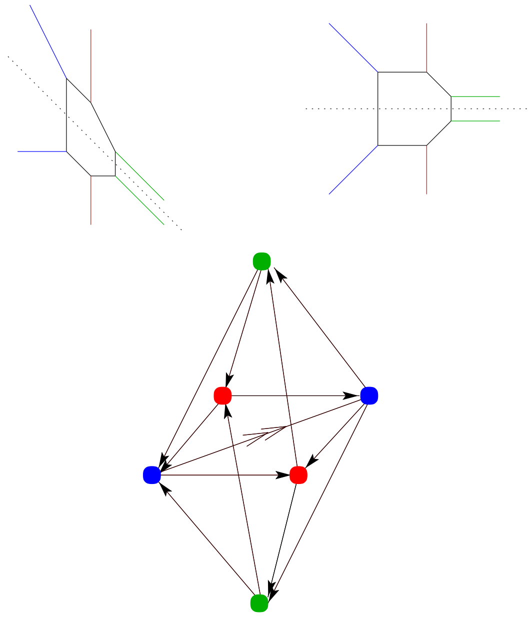

Figure 15: Two different (p, q) webs for phase II of dP_3. Once again, nodes of the same color transform into one another by the quiver symmetries.

$\mathbb{Z}_2$ **axial symmetries:** this is another example of symmetries that can be read directly from the (p, q) webs. They appear whenever the web has an axis of symmetry. In these cases the theories are invariant under exchange of gauge groups associated to external legs at both sides of the axis and charge conjugation of all fields. Is it important to notice that these reflections are indeed a subset of a larger set of transformations, given by all the $GL(2, \mathbb{Z})$ symmetries that map the webs onto themselves (i.e. that preserve the (p, q) charges of external legs). We have chosen to discuss $\mathbb{Z}_2$ reflections because they are the simplest of these symmetries, but we will also be considering the case of rotations later in this section. As an example, we present phase II of dP_3 in figure 15. The two webs in figure 15 are equivalent, and correspond to the same phase. We have presented both in order to illustrate how the same symmetry can arise in differently looking webs. Moreover, this example illustrates how the symmetry axis can sometimes be hidden. As it can be seen in the example, the axis can be made evident by an $\mathrm{SL}(2, \mathbb{Z})$ change of (p, q) basis, which preserves the intersection numbers between cycles and simply corresponds to a variation in the complex scalar τ in (2.1).

For this example,

$$\begin{aligned} e_1 &= (1,0) \qquad & e_1' &= (1,0) \\ e_2 &= (0,1) \qquad & e_2' &= (1,1) \end{aligned} \tag{5.1}$$

The two bases are related by the $\mathrm{SL}(2, \mathbb{Z})$ matrix

$$C = \begin{pmatrix} 1 & 1 \\ 0 & 1 \end{pmatrix} . \tag{5.2}$$

Based on the preceding observations, we can use the (p,q) webs listed in the appendix and make an immediate classification of the mentioned node symmetries that appear in each model. The results are summarized in table 1.

Singularity	Phase	Node Symmetry
F_0	I	$\mathbb{Z}_2 \times \mathbb{Z}_2$
	II	$\mathbb{Z}_2 \times \mathbb{Z}_2$
dP_0		D_3
dP_1		$\mathbb{Z}_2$
dP_2	I	$\mathbb{Z}_2$
	II	$\mathbb{Z}_2$
dP_3	I	D_6
	II	$\mathbb{Z}_2 \times \mathbb{Z}_2$
	III	$\mathbb{Z}_2 \times \mathbb{Z}_2$
	IV	D_6

Table 1: Classification of node symmetries.

Three of the models deserve a more detailed explanation. The first of them is dP_0, whose (p,q) web has an obvious $\mathbb{Z}_2$ axis of symmetry going along one of its legs. Furthermore, the three external legs are equivalent under $\mathrm{SL}(2,\mathbb{Z})$ transformations that "rotate" the web. As a result, the full node symmetry group of dP_0 is D_3. An identical reasoning applies to the first phase of dP_3, which has an evident $\mathbb{Z}_2$ axis, and whose six external legs are equivalent under $\mathrm{SL}(2,\mathbb{Z})$, leading to a D_6 symmetry. Finally, the fourth phase of dP_3 has one set of two and another one of three parallel external legs. According to our rules, this corresponds to a $\mathbb{Z}_2 \times S_3 = D_6$ symmetry.

6. Geometric transitions from the perspective of five dimensional theories

As we have discussed, (p,q) webs give a representation of the moduli space of $\mathcal{N}=1$ theories in 4 dimensions, for those cases in which the moduli space admits a toric description. For these models, brane webs are simply the toric skeletons representing vanishing cycles. At the same time, (p,q) webs can be used to study 5 dimensional $\mathcal{N}=1$ gauge theories living in the $4+1$ common dimensions of the branes. The purpose of this section will be to understand the translation of the four dimensional concepts of Seiberg duality and of different phases, to the five dimensional language. While doing so, we will get some nice dynamical information about the five dimensional theories.

6.1 Five dimensional interpretation of the theories

We have already discussed how (p,q) webs lead to 5 dimensional $\mathrm{SU}(N_c)$ theories with N_F flavors. The number of colors is given by the number of parallel internal branes. For all the cases we are studying, the (p,q) webs posses only one closed face (i.e. a single compact 4-cycle in the geometric interpretation), and have a pair of parallel internal branes, so they will be associated to SU(2) theories. In all the webs sketched in figures 6 to 11, it is possible to identify at least one such a pair of parallel finite branes that play the role of color branes.

Of the N_L external legs of a web, four have to be the supporting structure of color branes. It is also possible to see that in all the studied webs, after we identify the supporting branes, the remaining ones result to be parallel to color branes, thus admitting an interpretation as $N_F = N_L - 4$ flavor branes. Putting all these things together we see that F_0 phases will be associated to SU(2) with no flavors, while dP_n theories will be represented in five dimensions by SU(2) models with $N_F = n-1$.

There are two theories that require a more careful interpretation. The first one is the well-known case of dP_0. Having only three external legs, this theory is understood as SU(2) with -1 flavors. We can extend the reasoning in the following way, any time we face a theory where we cannot identify $N_L - 4$ legs as flavors, we blow up N points until reaching a model with the usual interpretation. This theory will have $N_L + N - 4$ flavors. Then we say that the number of flavors in the original theory is $(N_L + N - 4) - N$. The other special case is phase IV of dP_3, which is shown in figure 16 together with the same (p, q) web blown-up at one point. According to our previous statements, the five dimensional interpretation of this model is SU(2) with $3 - 1$ flavors.

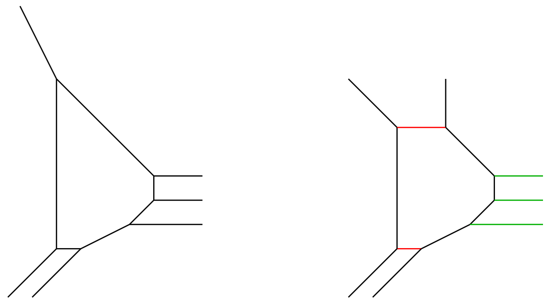

Figure 16: Phase IV of dP_3. It can be interpreted in five dimensions as SU(2) with 3-1 flavors.

6.2 Different limits in moduli space, a first example

Let us start studying how the flow between theories can be interpreted as adding a flavor to the corresponding five dimensional gauge theory and considering different, eventually infinite, limits in parameter space. To do so, let us focus on the example of a transition between one of the phases of F_0 and dP_1. The main point here is to realize that in both brane configurations one of the external legs can be understood as coming from a junction between two branes, one of which is a flavor brane. When taking the location of this junction very far away from the core of the (p, q) web, the configurations become those studied in sections 4.1 and 4.2. The position of the flavor brane is parametrized by the bare mass of the quark. When it becomes infinite, the quark decouples leaving us with pure SU(2) theories with no flavors.

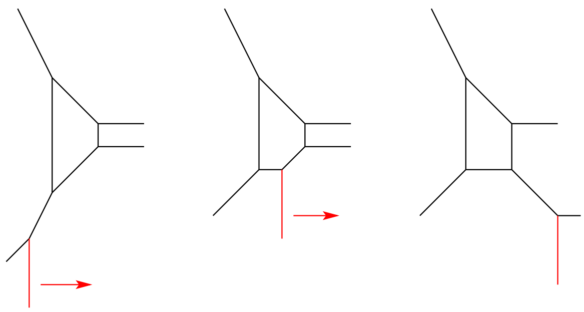

Figure 17: Flowing from F_0 to dP_1 by tuning the bare mass of the quark from $m \to -\infty$ to $m \to \infty$.

Figure 17 shows how in the limit $m \to -\infty$ we have the second phase of F_0, for $|m| < \phi/2$ we get phase I of dP_2 and finally we obtain dP_1 for $m \to \infty$.

6.3 Geometrical blow-ups as tuning bare masses

Encouraged by the example presented in the previous section, we can ask whether this is a general feature and we may indeed interpret all geometrical transitions of the type we are considering as tuning the bare mass for some quark. After inspecting figures 6 to 11 we conclude that this in fact is true!

The way of seeing this is that, in all cases, one of the two external legs connected to a 2-cycle coming from a blown-up point is parallel to a pair of finite segments in the

JHEP04(2003)043

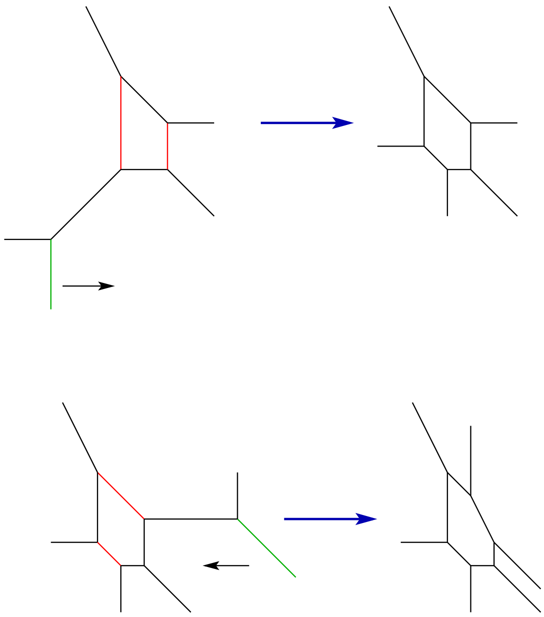

Figure 18: Flow $dP_1 \to dP_2\ II \to dP_3\ II$, obtained by bringing bare masses to finite values.

inner face of the (p, q) webs. Thus, this external leg can be understood as a flavor brane, while the two finite branes play the role of SU(2) color branes. We can think about the blowing-up process as bringing the flavor brane from infinity ($m \to \pm\infty$) until it reaches the body of the web. We can repeat this process indefinitely. One important point that has to be kept in mind is that, after each step, the two branes acting as color branes can change (and thus the orientation of the flavor brane we have to consider).

Figure 18 shows an example of a flow $dP_1 \to dP_2\ II \to dP_3\ II$, illustrating how the direction of color and flavor branes can change at each step. As an aside, this example also shows an interesting situation, the fact that at some point in the blow-up process there can be more than one possible choices of which branes to consider color branes. We see that, before the second blow-up, another legitimate choice would have been the two vertical finite branes.

6.4 BPS spectrum

BPS states in the five dimensional theory are given by webs of strings ending on the 5-brane web [14]. We will use this construction to see how BPS spectra of different phases are related. Let us consider the two phases of dP_2 since they constitute one of the simplest examples. We will also restrict our analysis to BPS states associated to string webs with only two and three end points (the extension to other states is immediate). The corresponding configurations are shown in figure 19.

Both spectra are quite different. Specifically there is no analog of state b of phase II in phase I. Nevertheless, we have seen that both the geometric picture and the five dimensional one in terms of varying parameters suggest that the passage between different phases is a continuous process.

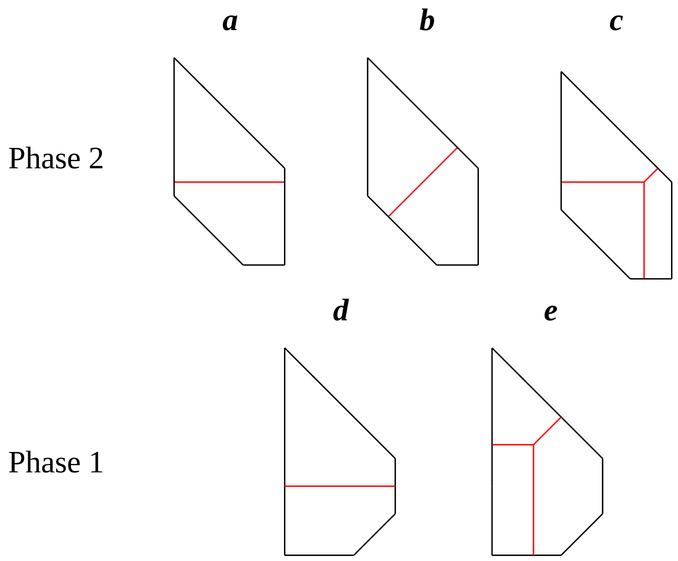

Figure 19: Some BPS states for phases I and II of dP_2. String junctions are represented in red. For simplicity, we have suppressed the external legs of the (p, q) webs.

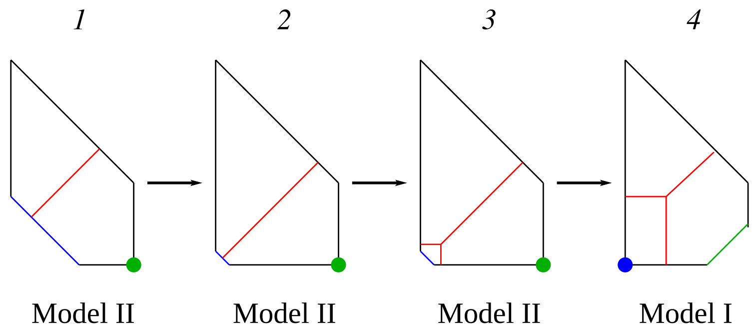

Figure 20: Continuous flow between BPS states of the two phases of dP_2.

Let us understand how the two spectra are continuously connected. To do so, we follow the fate of state b as we flow between phases II and I. In figure 20 we show different stages of this transition. The starting point is phase II and we gradually reduce the size of the blue 2-cycle. From stages 2 and 3 we see that, as the blue cycle approaches zero size, state b becomes degenerate with one state of type c (both of them in the BPS spectrum of phase II). State c survives the transition, becoming state e of phase I. The final step consists on shrinking the blue 2-cycle to a point and blowing up the green point. In conclusion state b undergoes a continuous transformation into state e, going through a point at which both states have the same mass.

We have understood that, for the specific case of geometric transitions between dP_2 phases, BPS states corresponding to string junctions with support on collapsing 2-cycles cease to exist as these 2-cycles shrink to a point, but become degenerate with other BPS states that remain in the spectrum. The same conclusion can be reached in the general case.

The string junctions (BPS states in five dimensions) that can in principle disappear abruptly are those ending on shrinking blown-up 2-cycles (exceptional curves). It is easy to see (and figures 6 to 11 illustrate this fact) that external legs attached to exceptional curves are parallel to internal branes ending on the corresponding segment of the (p, q) web. The general situation is presented in figure 21, where the charges of internal branes are shown between brackets, and those of external legs between parentheses.

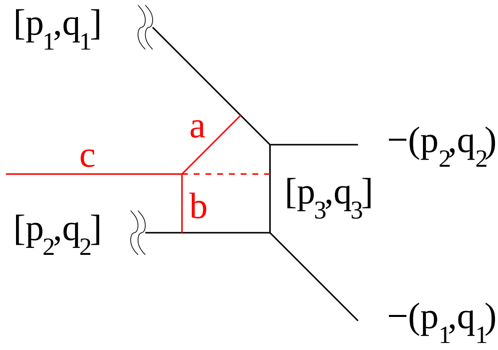

Figure 21: Continuous connection between BPS states in the general case.

(p, q) charge conservation fixes the slope of the shrinking brane to be given by

$$[p_3, q_3] = [p_1 - p_2, q_1 - q_2] \,. \tag{6.1}$$

Let us now consider the string junction shown in red in figure 21, which can be part of a larger BPS configuration. Its a and b legs are perpendicular to branes 1 and 2. Thus

$$\begin{aligned} (p_a, q_a) &= (q_1, -p_1) \\ (p_b, q_b) &= (-q_2, p_2) \end{aligned} \tag{6.2}$$

Once again, (p, q) charge conservation implies

$$(p_c, q_c) = (q_1 - q_2, -p_1 + p_2) = (q_3, -p_3) \tag{6.3}$$

Then, string c is perpendicular to brane 3. We can now follow a reasoning identical to the one used previously for dP_2. As brane 3 goes to zero size, legs a and b of the string junction can be negligible small, and the corresponding BPS state becomes degenerate with the one ending directly on brane 3. This concludes our proof of the continuity of BPS spectra in the general case.

We discussed in section 4.1 how Seiberg dual theories are related by the combination a blow-down and a blow-up in the non-compact Calabi-Yau probed by the D3-brane. The arguments presented in this section lead us to an important conclusion, Seiberg duality between theories in four dimensions, appears in the associated five dimensional models as crossing curves of marginal stability.

6.5 Continuity of the monopole tension

In this section we will calculate another five dimensional quantity, the monopole tension, and study how its values for different theories are related

Let us consider the example of the two phases of dP_2, which in five dimensional language correspond to SU(2) theories with one flavor. Calculating the monopole tensions for these two phases (which is simply the area of the inner face of the (p,q) web [14]) we find

$$\begin{aligned} T_M^{(I)} &= \frac{7}{8}\phi^2 + \left(\frac{1}{g_0^2} + \frac{m}{2}\right)\phi - \frac{m^2}{2} \\ T_M^{(II)} &= \frac{7}{8}\phi^2 + \frac{\phi}{g_0^2} - \frac{m^2}{2}\,. \end{aligned} \tag{6.4}$$

We see that this quantity has a different functional dependence on the parameters when we consider the two theories. Another question (whose answer is obvious from the (p,q) web picture) is what the value of $T_M^{(I)}$ is when $m = \phi/2$. In this situation we know that one of the quarks becomes massless, while the other one gets the same mass that the gauge boson $m_Q = \phi$. The tension in this case becomes

$$T_M = \phi^2 + \frac{\phi}{g_0^2} \tag{6.5}$$

which is exactly that for dP_1. Once again, the transition is continuous.

7. Conclusions

In this paper we have studied dualities and flows between gauge theories living on D3-branes probing toric singularities. We have found (p,q) webs very useful for this task, and for establishing relations among the probed geometry, the four dimensional theories on the world volume of the branes and five dimensional SU(2) associated theories.

In section 4 we have interpreted the flow between the four dimensional theories corresponding to the zeroth Hirzebruch and the del Pezzo surfaces as geometric transitions in the probed singularities. We also established the geometric transformations connecting toric dual models. In doing so, the (p,q) web representation of the toric varieties became not only a useful pictorial representation of the process, but a whole computational tool. The process of obtaining all the theories is reduced to doing successive blow-ups and to calculate intersection matrices. This simplicity can be contrasted with methods previously employed for the same task, based on partial resolutions of $\mathbb{C}^3/(\mathbb{Z}^3 \times \mathbb{Z}^3)$, which are computationally much more involved. Another advantage of the (p,q) web approach is that it offers a geometric intuition at every point of the process.

Furthermore, we studied the connection between blow-downs(ups) and (un)higgsings in the four dimensional theories. When doing so, the associated (p,q) webs permit the immediate identification of which field must acquire a non-zero vev. This was exemplified by getting the partial resolutions of $\mathbb{C}^3/(\mathbb{Z}^3 \times \mathbb{Z}^3)$ that give the four toric dual theories corresponding to dP_3.

Section 5 was devoted to study how quiver symmetries can be read off from (p,q) webs. The web constructions make these symmetries evident. The identification of the symmetry groups is reduced to counting parallel external legs and finding axes of symmetry.

In section 6 we initiated the exploration of a new perspective for geometric transitions. Exploiting the connection provided by (p,q) webs, we developed the interpretation of the studied theories as five dimensional SU(2) gauge theories with N_F flavors. We showed how geometrical blow-ups can be understood as bringing flavors from infinite bare mass. We proved that BPS spectra of two theories connected by a geometric transition are continuously connected. In this language, the transition corresponds to crossing a curve of marginal stability. We also studied the continuous relation between the monopole tensions in two such theories.

Acknowledgments

The authors would like to thank Bo Feng, Yang-Hui He and Amer Iqbal for valuable discussions. A.H. would like to thank the organizers of the "M Theory" workshop in the "Isaac Newton Institute for Mathematical Sciences" for their hospitality while this work was being completed. S.F. would also like to thank Martin Schvellinger for helpful conversations. Research supported in part by the CTP and the LNS of MIT and the U.S. Department of Energy under cooperative agreement #DE-FC02-94ER40818. A.H. is also supported by the Reed Fund Award and a DOE OJI award.

A. Gauge theories for branes on toric singularities

In this appendix we summarize the theories studied throughout the paper. For each of them we give a (p, q) web and its quiver.[3] For the del Pezzo surfaces, we also include the corresponding fractional brane charges. These charges were calculated with the procedure described in [16], which uses the map between 3-cycles in the mirror manifold and vector bundles on the del Pezzo surfaces of [20, 21]. The purpose of their inclusion is to exemplify how the combination and splitting of external legs of the (p, q) webs are associated to the same operations on the fractional brane charges.

Cone over F_0. F_0 has two phases. Phase I has 12 fields, while Phase II has 8.

(p,q) web	Quiver	Intersection matrix
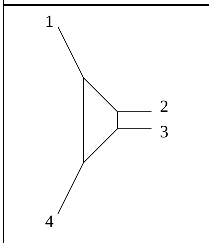	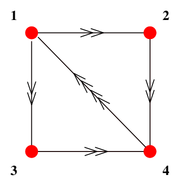	$\mathcal{I}_I = \begin{pmatrix} 0 & -2 & -2 & 4 \\ 2 & 0 & 0 & -2 \\ 2 & 0 & 0 & -2 \\ -4 & 2 & 2 & 0 \end{pmatrix}$
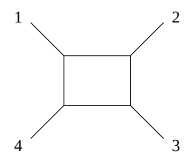	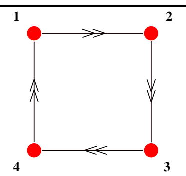	$\mathcal{I}_{II} = \begin{pmatrix} 0 & -2 & 0 & 2 \\ 2 & 0 & -2 & 0 \\ 0 & 2 & 0 & -2 \\ -2 & 0 & 2 & 0 \end{pmatrix}$

(A.1)

[3] In some of the quivers we have charge conjugated all the fields in order to follow the ones presented in the references [5, 6, 7, 9].

Cone over dP_0. dP_0 has one phase with 9 fields.

(p,q) web	Quiver	Intersection matrix	Fractional brane charges
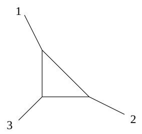	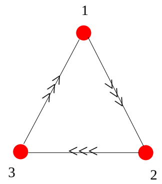	$\mathcal{I}=\begin{pmatrix} 0 & -3 & 3 \\ 3 & 0 & -3 \\ -3 & 3 & 0 \end{pmatrix}$	$ch(F_1) = (2,-\ell,-\frac{1}{2})$ $ch(F_2) = (-1,\ell,-\frac{1}{2})$ $ch(F_3) = (-1,0,0)$

(A.2)

Cone over dP_1. dP_1 has one phase with 10 fields.

(p,q) web	Quiver	Intersection matrix	Fractional brane charges
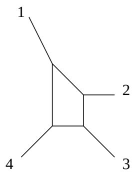	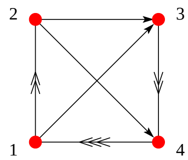	$\mathcal{I}=\begin{pmatrix} 0 & -2 & -1 & 3 \\ 2 & 0 & -1 & -1 \\ 1 & 1 & 0 & -2 \\ -3 & 1 & 2 & 0 \end{pmatrix}$	$ch(F_1) = (2,-\ell,-\frac{1}{2})$ $ch(F_2) = (0,E_1,-\frac{1}{2})$ $ch(F_3) = (-1,\ell-E_1,0)$ $ch(F_4) = (-1,0,0)$

(A.3)

Cone over dP_2. dP_2 has two phases, with 13 and 11 fields.

(p,q) web	Quiver	Intersection matrix	Fractional brane charges
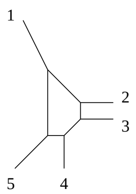	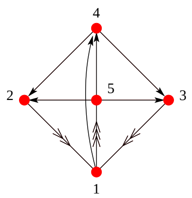	$\mathcal{I}_I=\begin{pmatrix} 0 & -2 & -2 & 1 & 3 \\ 2 & 0 & 0 & -1 & -1 \\ 2 & 0 & 0 & -1 & -1 \\ -1 & 1 & 1 & 0 & -1 \\ -3 & 1 & 1 & 1 & 0 \end{pmatrix}$	$ch(F_1)=(2,-\ell,-\frac{1}{2})$ $ch(F_2)=(0,E_1,-\frac{1}{2})$ $ch(F_3)=(0,E_2,-\frac{1}{2})$ $ch(F_4)=(-1,\ell-E_1-E_2,\frac{1}{2})$ $ch(F_5)=(-1,0,0)$
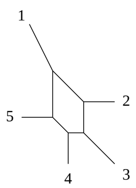	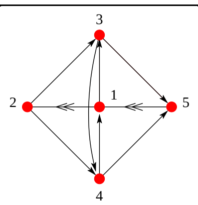	$\mathcal{I}_{II}=\begin{pmatrix} 0 & -2 & -1 & 1 & 2 \\ 2 & 0 & -1 & -1 & 0 \\ 1 & 1 & 0 & -1 & -1 \\ -1 & 1 & 1 & 0 & -1 \\ -2 & 0 & 1 & 1 & 0 \end{pmatrix}$	$ch(F_1)=(2,-\ell,-\frac{1}{2})$ $ch(F_2)=(0,E_1,-\frac{1}{2})$ $ch(F_3)=(-1,\ell-E_1,0)$ $ch(F_4)=(-1,E_2,\frac{1}{2})$ $ch(F_5)=(0,-E_2,-\frac{1}{2})$

(A.4)

JHEP04(2003)043

Cone over dP_3. dP_3 has four phases, with 12, 14, 14 and 18 fields.

(p,q) web	Quiver	Intersection matrix	Fractional brane charges
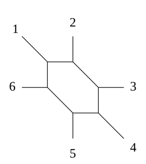	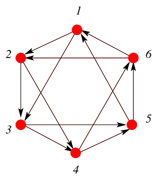	$\mathcal{I}_I = \begin{pmatrix} 0 & -1 & -1 & 0 & 1 & 1 \\ 1 & 0 & -1 & -1 & 0 & 1 \\ 1 & 1 & 0 & -1 & -1 & 0 \\ 0 & 1 & 1 & 0 & -1 & -1 \\ -1 & 0 & 1 & 1 & 0 & -1 \\ -1 & -1 & 0 & 1 & 1 & 0 \end{pmatrix}$	$ch(F_1) = (1, -\ell + E_3, 0)$ $ch(F_2) = (1, -E_3, -\frac{1}{2})$ $ch(F_3) = (0, E_1, -\frac{1}{2})$ $ch(F_4) = (-1, \ell - E_1, 0)$ $ch(F_5) = (-1, E_2, \frac{1}{2})$ $ch(F_6) = (0, -E_2, -\frac{1}{2})$
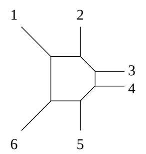	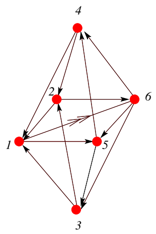	$\mathcal{I}_{II} = \begin{pmatrix} 0 & -1 & -1 & -1 & 1 & 2 \\ 1 & 0 & -1 & -1 & 0 & 1 \\ 1 & 1 & 0 & 0 & -1 & -1 \\ 1 & 1 & 0 & 0 & -1 & -1 \\ -1 & 0 & 1 & 1 & 0 & -1 \\ -2 & -1 & 1 & 1 & 1 & 0 \end{pmatrix}$	$ch(F_1) = (1, -\ell + E_3, 0)$ $ch(F_2) = (1, -E_3, -\frac{1}{2})$ $ch(F_3) = (0, E_1, -\frac{1}{2})$ $ch(F_4) = (0, E_2, -\frac{1}{2})$ $ch(F_5) = (-1, \ell - E_1$ $- E_2, \frac{1}{2})$ $ch(F_6) = (-1, 0, 0)$
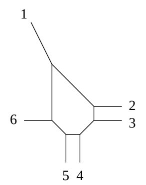	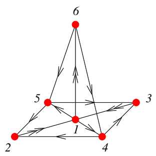	$\mathcal{I}_{III} = \begin{pmatrix} 0 & -2 & -2 & 1 & 1 & 2 \\ 2 & 0 & 0 & -1 & -1 & 0 \\ 2 & 0 & 0 & -1 & -1 & 0 \\ -1 & 1 & 1 & 0 & 0 & -1 \\ -1 & 1 & 1 & 0 & 0 & -1 \\ -2 & 0 & 0 & 1 & 1 & 0 \end{pmatrix}$	$ch(F_1) = (2, -\ell, -\frac{1}{2})$ $ch(F_2) = (0, E_1, -\frac{1}{2})$ $ch(F_3) = (0, E_3, -\frac{1}{2})$ $ch(F_4) = (-1, \ell - E_1$ $- E_3, \frac{1}{2})$ $ch(F_5) = (-1, E_2, \frac{1}{2})$ $ch(F_6) = (0, -E_2, -\frac{1}{2})$
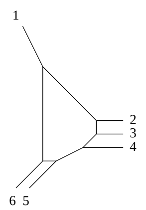	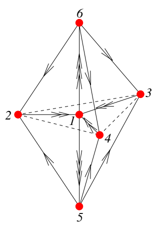	$\mathcal{I}_{IV} = \begin{pmatrix} 0 & -2 & -2 & -2 & 3 & 3 \\ 2 & 0 & 0 & 0 & -1 & -1 \\ 2 & 0 & 0 & 0 & -1 & -1 \\ 2 & 0 & 0 & 0 & -1 & -1 \\ -3 & 1 & 1 & 1 & 0 & 0 \\ -3 & 1 & 1 & 1 & 0 & 0 \end{pmatrix}$	$ch(F_1) = (2, -\ell, -\frac{1}{2})$ $ch(F_2) = (0, E_1, -\frac{1}{2})$ $ch(F_3) = (0, E_2, -\frac{1}{2})$ $ch(F_4) = (0, E_3, -\frac{1}{2})$ $ch(F_5) = (-1, \ell - E_1$ $- E_2 - E_3, 1)$ $ch(F_6) = (-1, 0, 0)$

(A.5)

References

[1] A. Hanany and E. Witten, *Type IIB superstrings, BPS monopoles and three-dimensional gauge dynamics*, *Nucl. Phys.* **B 492** (1997) 152 [hep-th/9611230].

[2] S. Katz, A. Klemm and C. Vafa, *Geometric engineering of quantum field theories*, *Nucl. Phys.* **B 497** (1997) 173 [hep-th/9609239];
S. Katz and C. Vafa, *Geometric engineering of $N = 1$ quantum field theories*, *Nucl. Phys.* **B 497** (1997) 196 [hep-th/9611090].

[3] M.R. Douglas and G.W. Moore, *D-branes, quivers and ALE instantons*, hep-th/9603167;
S. Kachru and E. Silverstein, *4d conformal theories and strings on orbifolds*, *Phys. Rev. Lett.* **80** (1998) 4855 [hep-th/9802183];
A.E. Lawrence, N. Nekrasov and C. Vafa, *On conformal field theories in four dimensions*, *Nucl. Phys.* **B 533** (1998) 199 [hep-th/9803015];
A. Hanany and A.M. Uranga, *Brane boxes and branes on singularities*, *J. High Energy Phys.* **05** (1998) 013 [hep-th/9805139].

[4] E. Witten, *Phases of $N = 2$ theories in two dimensions*, *Nucl. Phys.* **B 403** (1993) 159 [hep-th/9301042].

[5] B. Feng, A. Hanany and Y.-H. He, *D-brane gauge theories from toric singularities and toric duality*, *Nucl. Phys.* **B 595** (2001) 165 [hep-th/0003085].

[6] B. Feng, A. Hanany and Y.-H. He, *Phase structure of D-brane gauge theories and toric duality*, *J. High Energy Phys.* **08** (2001) 040 [hep-th/0104259].

[7] B. Feng, A. Hanany, Y.-H. He and A.M. Uranga, *Toric duality as Seiberg duality and brane diamonds*, *J. High Energy Phys.* **12** (2001) 035 [hep-th/0109063].

[8] C.E. Beasley and M.R. Plesser, *Toric duality is Seiberg duality*, *J. High Energy Phys.* **12** (2001) 001 [hep-th/0109053].

[9] B. Feng, S. Franco, A. Hanany and Y.-H. He, *Symmetries of toric duality*, *J. High Energy Phys.* **12** (2002) 076 [hep-th/0205144].

[10] T. Muto, *D geometric structure of orbifolds*, hep-th/0206012.

[11] F. Cachazo, B. Fiol, K.A. Intriligator, S. Katz and C. Vafa, *A geometric unification of dualities*, *Nucl. Phys.* **B 628** (2002) 3 [hep-th/0110028].

[12] B. Feng, A. Hanany, Y.H. He and A. Iqbal, *Quiver theories, soliton spectra and Picard-Lefschetz transformations*, *J. High Energy Phys.* **02** (2003) 056 [hep-th/0206152].

[13] O. Aharony and A. Hanany, *Branes, superpotentials and superconformal fixed points*, *Nucl. Phys.* **B 504** (1997) 239 [hep-th/9704170].

[14] O. Aharony, A. Hanany and B. Kol, *Webs of (p,q) 5-branes, five dimensional field theories and grid diagrams*, *J. High Energy Phys.* **01** (1998) 002 [hep-th/9710116].

[15] N.C. Leung and C. Vafa, *Branes and toric geometry*, *Adv. Theor. Math. Phys.* **2** (1998) 91 [hep-th/9711013].

[16] A. Hanany and A. Iqbal, *Quiver theories from D6-branes via mirror symmetry*, *J. High Energy Phys.* **04** (2002) 009 [hep-th/0108137].

[17] W. Fulton *Introduction to toric varieties*, Princeton University Press, 1993.

[18] P.S. Aspinwall, *Resolution of orbifold singularities in string theory*, hep-th/9403123;
M.R. Douglas, B.R. Greene and D.R. Morrison, *Orbifold resolution by D-branes*, *Nucl. Phys.* **B 506** (1997) 84 [hep-th/9704151];
D.R. Morrison and M.R. Plesser, *Non-spherical horizons, I*, *Adv. Theor. Math. Phys.* **3** (1999) 1 [hep-th/9810201];
C. Beasley, B.R. Greene, C.I. Lazaroiu and M.R. Plesser, *D3-branes on partial resolutions of abelian quotient singularities of Calabi-Yau threefolds*, *Nucl. Phys.* **B 566** (2000) 599 [hep-th/9907186].

[19] K. Hori and C. Vafa, *Mirror symmetry*, hep-th/0002222;
K. Hori, A. Iqbal and C. Vafa, *D-branes and mirror symmetry*, hep-th/0005247.

[20] T. Hauer and A. Iqbal, *Del pezzo surfaces and affine 7-brane backgrounds*, *J. High Energy Phys.* **01** (2000) 043 [hep-th/9910054].

[21] K. Mohri, Y. Ohtake and S.-K. Yang, *Duality between string junctions and D-branes on del Pezzo surfaces*, *Nucl. Phys.* **B 595** (2001) 138 [hep-th/0007243].

[22] B. Feng, S. Franco, A. Hanany and Y.-H. He, *Unhiggsing the del Pezzo*, hep-th/0209228.

JHEP04(2003)043